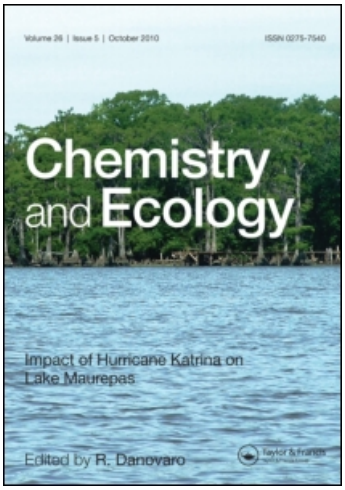

Chemistry and Ecology
Publication details, including instructions for authors and subscription information:
http://www.informaworld.com/smpp/title~content=t713455114

Removal of Cr(VI) from aqueous solution using waste weed, *Salvinia cucullata*

S. S. Baral[a]; S. N. Das[a]; P. Rath[b]; G. Roy Chaudhury[a]; Y. V. Swamy[a]
[a] Department of Biomineral Processing & Environmental Management, Regional Research Laboratory (CSIR), Bhubaneswar, India [b] Department of Chemical Engineering, National Institute of Technology, Rourkela, India

To cite this Article Baral, S. S. , Das, S. N. , Rath, P. , Chaudhury, G. Roy and Swamy, Y. V.(2007) 'Removal of Cr(VI) from aqueous solution using waste weed, *Salvinia cucullata*', Chemistry and Ecology, 23: 2, 105 — 117
To link to this Article: DOI: 10.1080/02757540701197697
URL: http://dx.doi.org/10.1080/02757540701197697

Chemistry and Ecology
Vol. 23, No. 2, April 2007, 105–117

Taylor & Francis
Taylor & Francis Group

Removal of Cr(VI) from aqueous solution using waste weed, *Salvinia cucullata*

S. S. BARAL†, S. N. DAS†, P. RATH‡, G. ROY CHAUDHURY*† and Y. V. SWAMY†

†Department of Biomineral Processing & Environmental Management, Regional Research Laboratory (CSIR), Bhubaneswar 751013, India
‡Department of Chemical Engineering, National Institute of Technology, Rourkela 769008, India

(Received 2 August 2006; in final form 10 December 2006)

Biosorption studies of Cr(VI) were carried out using waste weed, *Salvinia cucullata*. Various adsorption parameters were studied, such as agitation speed, contact time, pH, particle size, and concentrations of adsorbent and adsorbate. The equilibrium was achieved in 12 h. A lower pH favoured adsorption of Cr(VI). The kinetics followed pseudo-second-order rate equations. The adsorption isotherm obeyed both the Langmuir and Freundlich models. The calculated activation energy (1.1 kJ mol^{-1}) suggested that the adsorption followed a diffusion-controlled mechanism. Various thermodynamic parameters such as ΔG°, ΔH°, and ΔS° were also calculated. The positive values of enthalpy indicated the endothermic nature of the reaction, and ΔS° showed the increasing randomness at the solid liquid interface of Cr(VI) on the adsorbent, which revealed the ease of adsorption reaction. These thermodynamic parameters showed the spontaneity of the reaction. The maximum adsorption of uptake (232 mg g^{-1}) compared well with reported values of similar adsorbents. The rate-determining step was observed to follow an intra-particle diffusion model.

Keywords: Weed; Adsorption; Equilibrium; Isotherm; Kinetics; Rate-determining step

1. Introduction

Chromium and its salts have many industrial uses such as electroplating, alloying, leather tanning, corrosion protection, etc. [1]; therefore, their demand is increasing with time. The waste and effluent streams of chromite mining and processing units contain chromium in two oxidation states, i.e. Cr(VI) and Cr(III), in aqueous solution. As Cr(VI) species is mobile, its oxidizing character is regarded as potentially carcinogenic [2]. On the other hand, Cr(III) hydroxide has limited solubility in the aqueous phase and is thus regarded as a non-dangerous pollutant.

Abatement of pollution due to Cr(VI) mainly consists of two main processes: reduction of Cr(VI) to Cr(III) to render it harmless, and removal of Cr(VI) as such. The reduction

*Corresponding author. Email: groychaudhury@rrlbhu.res.in

Chemistry and Ecology
ISSN 0275-7540 print/ISSN 1029-0370 online © 2007 Taylor & Francis
http://www.tandf.co.uk/journals
DOI: 10.1080/02757540701197697

followed by precipitation technique [3] is widely used for the treatment of wastewater containing Cr(VI), although the process suffers from several drawbacks such as solid–liquid separation and disposal of sludge. Alternate methods are now being developed to treat Cr(VI)-contaminated wastewater using various techniques such as adsorption, ion exchange, and membrane separation. The membrane system has problems like scaling, fouling, and blocking. The ion-exchange system is uneconomic due to the cost of commercial ion-exchange resins. The adsorption technique is economically favourable and technically easy to separate as the requirement of the control system is minimum [4]. In recent years, a number of low-cost non-conventional adsorbents have been used to treat Cr(VI)-contaminated wastewater [5–11].

Keeping in view the importance of abatement of pollution due to Cr(VI) in wastewater, in the present study a waste weed, *Salvinia cucullata*, growing profusely in sweet water ponds and lakes was used to adsorb Cr(VI) from synthetic aqueous solutions and evaluate the efficiency of the technique. The main objective of the study is to develop a cheap and convenient process so that the people in remote/rural areas may be able to treat Cr(VI)-contaminated water for drinking and household purposes. The adsorption efficiency of the adsorbent was studied as a function of pH, adsorbate concentration, adsorbent dose, temperature, agitation speed, and particle size. Different adsorption isotherms were used to determine the best fit to the experimental data by using the average absolute percentage deviation between the experimental and predicted uptake. The thermodynamics parameters were calculated to determine the feasibility of the adsorption process.

2. Material and methods

2.1 *Experimental*

The adsorbent, *Salvinia cucullata*, a waste weed used in this study, was collected from a lake at Nandan Kanan, situated about 15 km from Bhubaneswar. The weed was washed with distilled water, followed by sun-drying and finally drying in an oven at 70 °C for 4 h. The dried weed was ground and sieved to obtain different sieve fractions, and the size analysis was carried out using a Malvern Particle Size Analyzer model-2000.

Adsorption experiments were carried out in 100-ml beakers using 50 ml of synthetic Cr(VI) solution. Aqueous solution of Cr(VI) was prepared by dissolving the requisite amount of $K_2Cr_2O_7$ in deionized water. A stock solution with a Cr(VI) concentration of 1000 mg l^{-1} was prepared and subsequently diluted to the required strengths for the adsorption studies. The mixtures were stirred by a mechanical stirrer. Adsorption studies were carried out at different temperatures using an automatic temperature-controlled water bath with an accuracy of ± 0.5 °C. The pH of the solution was adjusted before mixing the adsorbent, by using dilute HCl or NaOH, as appropriate. After adsorption, the mixture was filtered through Whatman No. 42 filter paper. The residual Cr(VI) concentration was determined by the diphenylcarbazide method, using an UV/visible spectrophotometer (Perkin Elmer Lambda-35) [12]. For the FT-IR study, 2 mg of finely ground adsorbent and Cr(VI) loaded materials was taken separately. KBr (400 mg; spectroscopy grade) was mixed separately with each sample and pressed to prepare translucent sample disks. All experiments were carried out using AR/GR-grade EMerck chemicals. Deionized water was used for the preparation and colorimetric analysis of Cr(VI) solution. All experiments were carried out in duplicate, and the average of the two are shown in the results. The differences between duplicate experimental values were in the range of $\pm 3\%$.

3. Results and discussion

3.1 *Effect of agitation speed*

Adsorption studies were carried out at varying agitation speeds: 100–800 rpm. It was observed that the percentage of adsorption increases with increasing stirring speed up to 600 rpm (figure 1), and thereafter the adsorption efficiency is independent of agitation speed. The increase in adsorption efficiency with the increase in agitation could be mainly due to resistance to mass transport in the bulk solution at lower agitation speeds. A thin liquid film surrounding the adsorbent particles offered resistance to mass transport by diffusion. As the agitation speed increased, there would be a decrease in the thickness of the boundary film, thereby decreasing the effect of film diffusion. Since beyond an agitation speed of 600 rpm, there was hardly any increase in adsorption efficiency, further studies were carried out with this agitation speed. Under these experimental conditions, it can be safely assumed that solution homogeneity can be maintained, and simultaneously there may be no appreciable attrition of the adsorbent particle during the adsorption process.

3.2 *Effect of contact time*

Contact time is an important parameter to determine the process parameter. To determine the minimum contact time required for maximum adsorption, studies were carried out for 12 h, and the results are shown in figure 2. It was observed that the kinetics could be divided into two parts: the initial faster reaction followed by a slower rate. The initial transfer rate usually

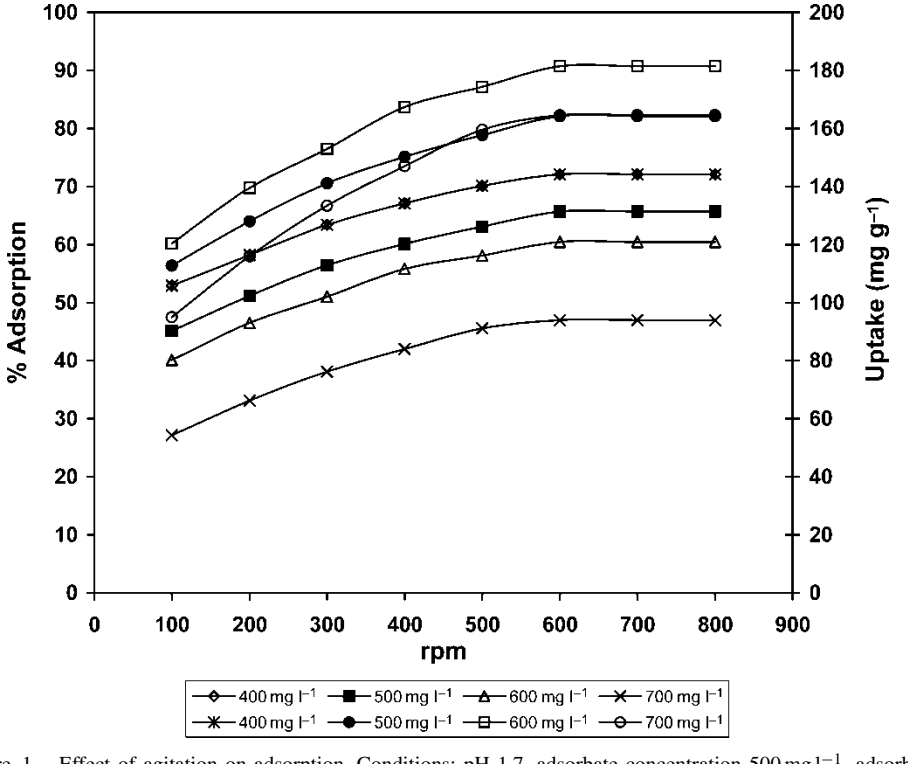

Figure 1. Effect of agitation on adsorption. Conditions: pH 1.7, adsorbate concentration 500 mg l^{-1}, adsorbent concentration 2 g l^{-1}, temperature 30 °C, time 12 h, particle size 53.55 μm.

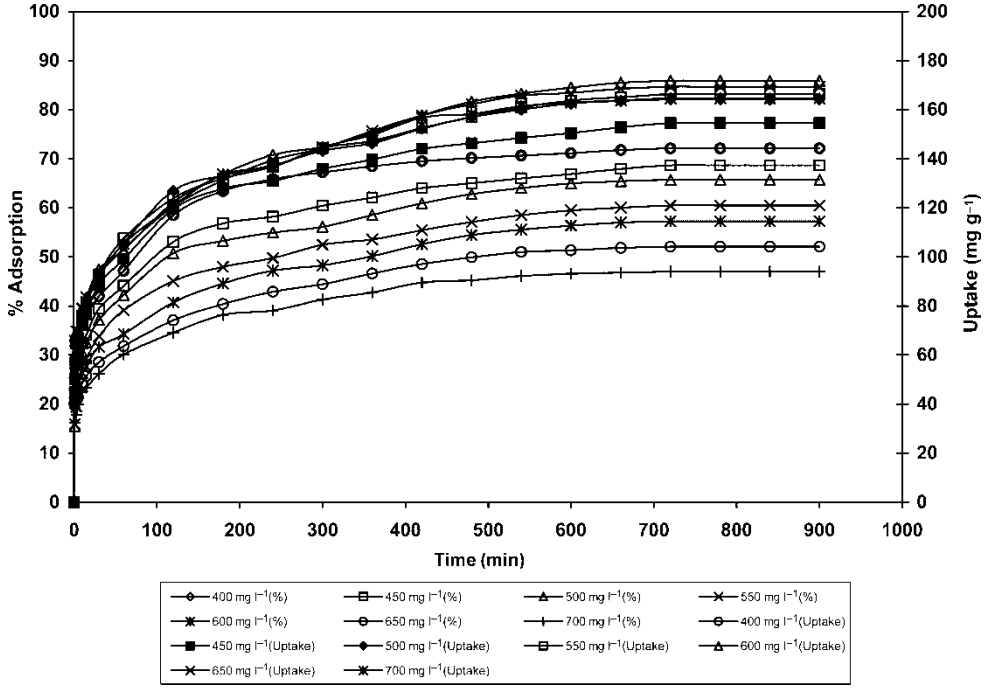

Figure 2. Effect of contact time on adsorption. Conditions: pH 1.7, adsorbate concentration 500 mg l^{-1}, adsorbent concentration 2 g l^{-1}, temperature 30 °C, agitation speed 600 rpm, particle size 53.55 μm.

lasted for 15 min, which accounted for >50% of total adsorption. As the reaction equilibrium was achieved in 12 h, all further studies were carried out using the optimum time.

3.3 *Effect of pH*

pH is another important parameter with which to determine the efficiency of adsorption. A number of experiments were carried out by varying the initial pH from 1.7 to 4.5, and the results are shown in figure 3. It was observed that in all cases, the equilibrium pH was higher than the initial pH, which indicated an acid neutralization effect and proton adsorption of the hydroxylated mineral surface, popularly known as the liquid exchange mechanism [13–15]. It is widely believed that the mechanism for the adsorption of anion onto adsorbent surface involves a surface-complexation phenomenon. There are two types of surface complexation: inner and outer complexation. The formation of these types of complexation depends on the degree of surface protonation or dissociation as shown below:

$$\equiv \mathrm{SOH(s)} + \mathrm{H^+} \Longleftrightarrow \equiv \mathrm{SOH_2^+(s)} \quad (1)$$

$$\equiv \mathrm{SOH(s)} \Longleftrightarrow \equiv \mathrm{SO^-(s)} + \mathrm{H^+}, \quad (2)$$

where ≡ SOH(s) is the surface of the adsorbent.

If there are more protonated surface groups than dissociated groups, the surface would be positively charged, thus facilitating anion adsorption. On the other hand, if the amounts of both species are equal, the net charge would be zero. Thus, the complex formation reaction

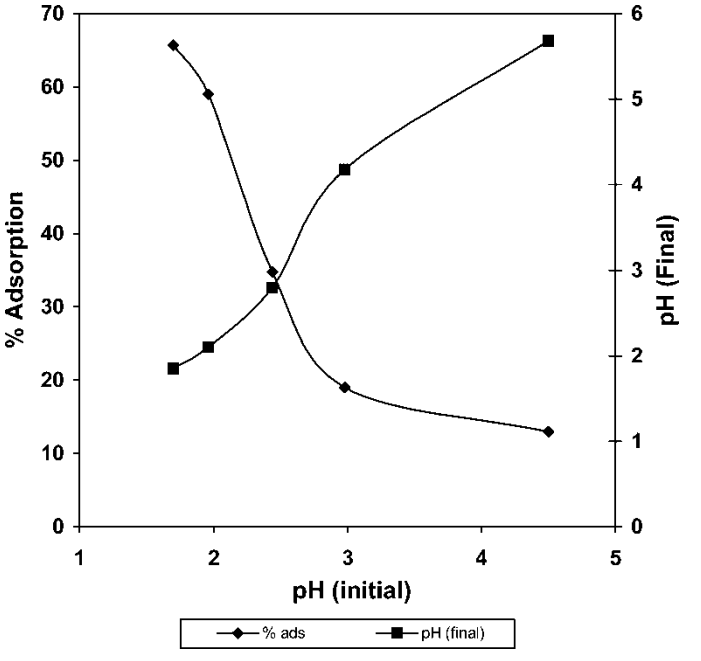

Figure 3. Effect of pH on adsorption. Conditions: Time 12 h, adsorbate concentration 500 mg l^{-1}, adsorbent concentration 2 g l^{-1}, temperature 30 °C, agitation speed 600 rpm, particle size 53.55 μm.

can be shown as follows:

$$\text{Outer sphere complex} : \equiv \text{SOH}_2^+(\text{s}) + \text{A}^{-n} \Longleftrightarrow \equiv \text{SOH}_2^+(\text{s}) - \text{A}^{-n}. \tag{3}$$

$$\text{Inner sphere complex} : \equiv \text{SOH}_2^+(\text{s}) + \text{A}^{-n} \Longleftrightarrow \equiv \text{SA}^{(n-1)}(\text{s}) + \text{H}_2\text{O}, \tag{4}$$

where A^{-n} is the anion, in the present case Cr(VI).

From the stability diagram [16], it can be seen that most dominant species in the aqueous solution are $HCrO_4^-$, CrO_4^{2-} and $Cr_2O_7^{2-}$, whereas the dominant species in pH range 1.7–4.5 (as in case of the present studies) is $HCrO_4^-$. An increase in the initial pH would convert $HCrO_4^-$ to CrO_4^{2-}. It was observed that a lower initial pH facilitated the adsorption of Cr(VI). The percentage of adsorption decreased slightly when the initial pH increased from 1.7 to 2, but beyond this, the adsorption efficiency decreased sharply. The increase in equilibrium pH was considerably lower at a lower initial pH compared with a higher initial pH, which indicates protonation of the adsorbent. The lower adsorption efficiency at a higher initial pH may be due to a decrease in net positive charge and competition between OH^- and $HCrO_4^-$ ions. Therefore, at higher pH values, there was a minor change in equilibrium pH, as shown in figure 3. The equilibrium time increased with pH as the efficiency of adsorption increased, while at a lower pH, the efficiency of adsorption was very high.

Again, the adsorption may be occurring due to the formation of complex with the chelating agent present in the adsorbent. Evidence of complex formation was obtained from Fourier transform infrared spectroscopy. Results show that the adsorbent contain two or more functional groups. The main absorbance bands for weed as such were: two sharp peak at 3350 cm^{-1} (H bonds, OH group) and 2930 cm^{-1} (aliphatic); three broad bands at 1630 cm^{-1} (unsaturated C=C), 1420 cm^{-1} (C−O stretch), and 1020 cm^{-1} (C−O stretch, Si−O stretch); and two small peaks at 1560 cm^{-1} (amide = bond) and 880 cm^{-1} (aromatic CH). The Cr(VI) adsorbed material showed either a shift or reduction in absorption peak, suggesting the vital role played by the functional group.

3.4 *Variation of initial Cr(VI) concentration*

The initial Cr(VI) concentration was varied from 400 to 700 mg l^{-1} to evaluate its effect on adsorption efficiency. It was observed that with the increase in initial concentration, the percentage of adsorption decreased, as is generally expected in the equilibrium process. When the initial concentration increased from 400 to 700 mg l^{-1}, the percentage of adsorption decreased from 72 to 47%, as shown in figure 4. The metal uptake capacity increased from 144 to 171 mg g^{-1} when the initial concentration increased from 400 to 600 mg l^{-1}. It decreased slightly when the initial metal ion concentration increased beyond 600 mg l^{-1}. This may be attributed to a higher availability of Cr(VI) ions in the solution. Moreover, a higher initial concentration provides an increased driving force to overcome the mass-transfer resistance of metal ions between the aqueous and solid phases, resulting in a higher probability of collision between Cr(VI) ion and the adsorbent. The decrease in uptake capacity beyond the Cr(VI) concentration of 600 mg l^{-1} may be due to saturation.

3.5 *Variation of adsorbent concentration*

The adsorbent concentration was varied from 0.8 to 2.4 g l^{-1} in order to determine the optimum adsorption efficiency. It was observed that the uptake decreased from 188 to 145 mg g^{-1} when the adsorbent concentration increased from 0.8 to 2.4 g l^{-1}. The percentage adsorption increased from 30 to 70% when the adsorbent concentration increased from 0.8 to 2.4 g l^{-1}. The results are shown in figure 5.

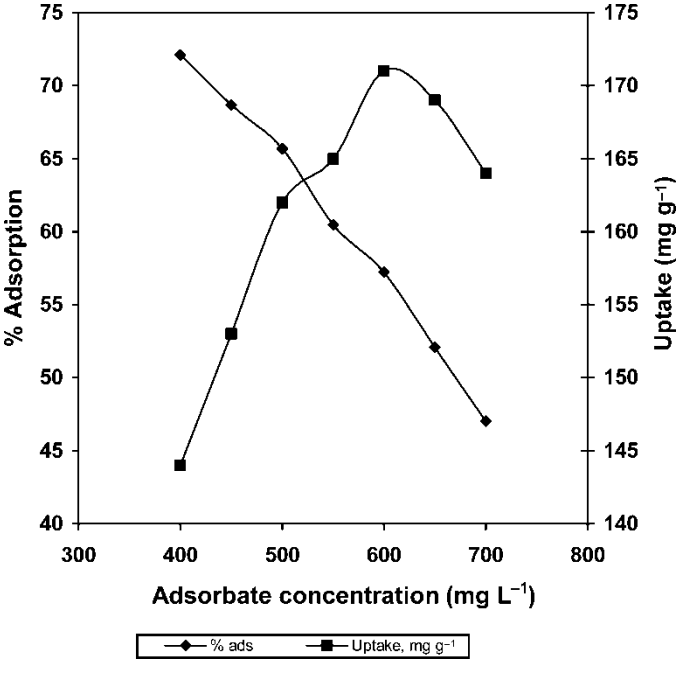

Figure 4. Effect of adsorbate concentration on adsorption. Conditions: time 12 h, pH 1.7, adsorbent concentration 2 g l^{-1}, temperature 30 °C, agitation speed 600 rpm, particle size 53.55 μm.

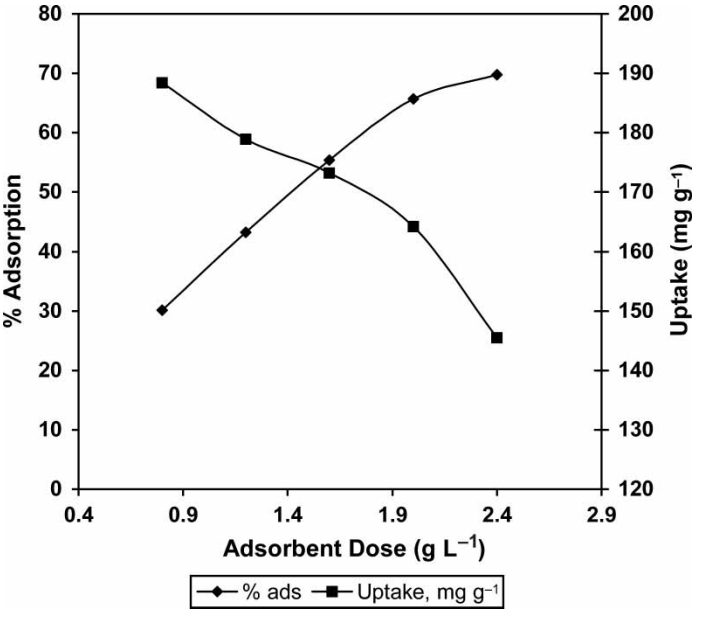

Figure 5. Effect of adsorbent dose on adsorption. Conditions: time 12 h, pH 1.7, adsorbate concentration 500 mg l^{-1}, temperature 30 °C, agitation speed 600 rpm, particle size 53.55 μm.

3.6 *Variation of temperature*

Temperature is also an essential parameter in determining the kinetics as the wastewater temperature varies widely. The temperature was varied from 30 to 60 °C, and the results are shown in figure 6. The uptake and the percentage adsorption increased almost in parallel with the increase in adsorption temperature. The percentage of adsorption and uptake increased from 65 to 84% and 164 to 212 mg g^{-1}, respectively, when the temperature increased from

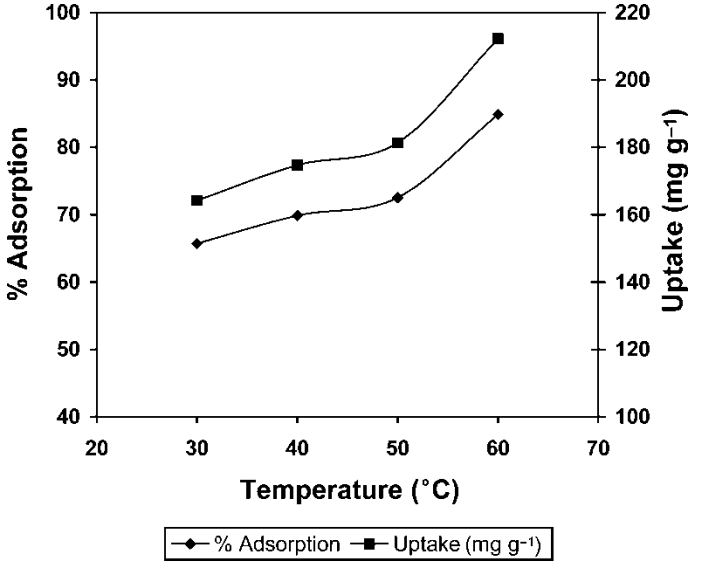

Figure 6. Effect of temperature on adsorption. Conditions: time 12 h, pH 1.7, adsorbate concentration 500 mg l^{-1}, adsorbent concentration 2 g l^{-1}, agitation speed 600 rpm, particle size 53.55 μm.

30 to 60 °C. The increase in efficiency with increase in temperature indicates that the reaction followed an endothermic pathway.

3.7 *Variation of particle size of adsorbent*

The particle size of the adsorbent was varied from 53 to 221 μm in order to determine the optimum particle size for maximal Cr(VI) removal. The results are shown in figure 7. The percentage adsorption decreased from 65 to 51% with increasing particle size from 53 to 221 μm, whereas the uptake decreased from 164 to 128 mg g^{-1}. The decrease in percentage of adsorption and uptake with increase in particle size may be attributed to the decrease in specific surface area of the adsorbent.

3.8 *Evaluation of rate equation*

In order to determine a suitable kinetic model, the adsorption data were fitted into the following three kinetics equations [17]:

(1) first order reversible;
(2) pseudo-first order;
(3) pseudo-second order.

The first-order reversible equation can be written as:

$$\ln(1 - U_t) = -k_r t \tag{5}$$

where $U_t = (C_{A0} - C_A)/(C_{A0} - C_{Ae}) = X_A/X_{Ae}$; $k_r = k_1(1 + 1/K_c) = k_1 + k_2$; $K_c = C_{Be}/C_{Ae} = k_1/k_2$.

Here, C_{A0} is the initial concentration, C_A is the concentration at time t, and C_{Ae} is the equilibrium adsorbate concentration in the solution; k_1 and k_2 are the rate constant, and K_c is the equilibrium constant.

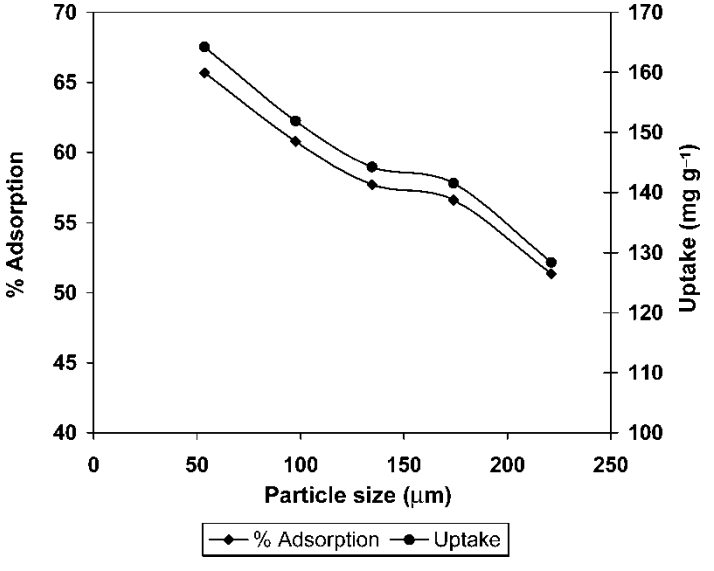

Figure 7. Effect of particle size on dsorption. Conditions: time 12 h, pH 1.7, adsorbate concentration 500 mg l^{-1}, adsorbent concentration 2 g l^{-1}, agitation speed 600 rpm, temperature 30 °C.

The values of the respective k_r were calculated by plotting $\ln(1 - U_t)$ vs t. k_1, k_2, and K_c were calculated using the above equations.

The pseudo-first-order reversible reaction can be written as:

$$\log(q_e - q) = \log(q_e) - k_1 t/2.303, \tag{6}$$

where q_e (mg g^{-1}) is the amount of solute adsorbed at equilibrium per unit weight of adsorbent, q (mg g^{-1}) is the amount of solute adsorbed at any time, and k_1 is the adsorption constant. The values of k_1 were calculated for different parameters from the slope of the linear graphs between $\log(q_e - q)$ vs t.

The pseudo-second-order reaction can be written as:

$$t/q = 1/k_2 q_e^2 + t/q_e, \tag{7}$$

where q_e, q, and k_2 have their usual meanings as for equation (6), and the values of k_2 were calculated from the intercept of the linear graph between t/q vs t.

Table 1 shows the specific reaction constant along with R^2 values. From R^2 and equilibrium concentration values for different parameters, it can be concluded that the adsorption follows pseudo-second-order kinetics.

Table 1. Evaluation of different kinetic equations: reaction kinetics model with different parameters.

	First order reversible					Pseudo-first order		Pseudo-second order		
Parameter	K_c	k_r	k_1	k_2	R^2	k	R^2	h	k	R^2
pH										
4.5	0.074659	0.0049	0.00034	0.00456	0.8291	0.005297	0.7684	0.2108	0.004497	0.998
3	0.116707	0.0033	0.000345	0.002955	0.922	0.003685	0.8354	0.316	0.001414	0.9875
2.44	0.267462	0.0056	0.001182	0.004418	0.9556	0.005988	0.9076	0.1436	0.000917	0.9904
1.96	0.718354	0.0046	0.001923	0.002677	0.9641	0.004836	0.9207	0.1087	0.000423	0.9905
1.7	0.957124	0.0049	0.002396	0.002504	0.9294	0.005297	0.8944	0.0801	0.000463	0.9969
Adsorbent concentration (ppm)										
400	1.385459	0.007	0.004066	0.002934	0.9826	0.005527	0.9183	0.0845	0.000496	0.9963
450	1.023297	0.0052	0.00263	0.00257	0.9294	0.00737	0.9535	0.0884	0.000544	0.9959
500	0.957124	0.0049	0.002396	0.002504	0.9477	0.005297	0.8944	0.0801	0.000463	0.9969
550	0.765063	0.0049	0.002124	0.002776	0.9778	0.005297	0.912	0.0851	0.000425	0.996
600	0.669333	0.0045	0.001804	0.002696	0.9872	0.004836	0.9196	0.086	0.000394	0.9959
650	0.543583	0.0047	0.001655	0.003045	0.978	0.005067	0.9333	0.0889	0.000393	0.9932
700	0.443599	0.0052	0.001598	0.003602		0.005527	0.9362	0.0872	0.000424	0.9943
Adsorbent dose (mg l^{-1})										
2.4	0.963636	0.0057	0.002797	0.002903	0.9792	0.005988	0.9386	0.1355	0.000348	0.9952
2	0.957124	0.0049	0.002396	0.002504	0.9294	0.005297	0.9021	0.1394	0.000266	0.9922
1.6	0.776806	0.0044	0.001924	0.002476	0.9518	0.004836	0.9096	0.1453	0.000229	0.9899
1.2	0.633928	0.0044	0.001707	0.002693	0.9588	0.004606	0.9163	0.1537	0.000201	0.9872
0.8	0.539549	0.0076	0.002663	0.004937	0.9798	0.00783	0.9727	0.1337	0.000211	0.9945
Temperature (°C)										
30	0.957124	0.0049	0.002396	0.002504	0.9294	0.004836	0.9294	0.0801	0.000463	0.9969
40	1.159365	0.0043	0.002309	0.001991	0.9671	0.004376	0.9663	0.0689	0.000476	0.9959
50	1.32073	0.0044	0.002504	0.001896	0.9572	0.004376	0.9533	0.0592	0.000514	0.9969
60	2.810323	0.0053	0.003909	0.001391	0.9871	0.005297	0.9871	0.0722	0.000307	0.9925
Particle size (μm)										
53.545	0.957124	0.0049	0.002396	0.002504	0.9294	0.004836	0.9294	0.0801	0.000463	0.9969
97.648	0.77464	0.0069	0.003012	0.003888	0.9884	0.006909	0.9894	0.1012	0.000428	0.9922
134.516	0.682487	0.0092	0.003732	0.005468	0.974	0.009212	0.9748	0.1113	0.000432	0.9899
173.942	0.652375	0.0094	0.003711	0.005689	0.901	0.009442	0.9818	0.1237	0.000404	0.9896
221.183	0.52773	0.0095	0.003282	0.006218	0.9352	0.009442	0.9352	0.0874	0.000694	0.9978

3.9 *Evaluation of thermodynamic parameters*

As discussed earlier, the adsorption process is more favourable at higher temperatures. The energy of activation was calculated to be 1.2 kJ mol^{-1}. From the value of activation energy, it appears that Cr(VI) adsorption on the weed is a physical adsorption as the activation energy is not more than 6 kJ mol^{-1} [18].

The standard free energy change, ΔG°, was calculated using the following relationship:

$$\Delta G^\circ = -RT \ln b, \tag{8}$$

where b is the Langmuir constant; T is the absolute temperature; and R is the gas constant.

The other thermodynamic parameters such as the change in standard enthalpy (ΔH°) and standard entropy (ΔS°) were determined using equation (9):

$$\ln k = \Delta S^\circ / R - \Delta H^\circ / T. \tag{9}$$

ΔS° and ΔH° were obtained from the slope and intercept of the Vant Hoff plot of $\ln k$ vs $1/T$ (Figure not shown). The calculated ΔH° and ΔS° values were 27.9 kJ mol^{-1} and 90.7 J mol^{-1}, respectively. The positive values of enthalpy indicate the endothermic nature of the reaction. The positive value of ΔS° shows the increasing randomness at the solid–liquid interface of Cr(VI) ions on the adsorbent.

3.10 *Evaluation of rate-determining steps*

Due to the porous nature of the adsorbent used in this study, pore diffusion is also expected, in addition to surface adsorption. The contact-time-variation experiments can be used to study the rate-determining step in the adsorption process [19]. Since the particles were agitated at a speed of 600 rpm, it can be safely assumed that the rate is not limited by mass transfer from the bulk liquid to the external surface of the particle. Therefore, the rate-determining step may be either film or intra-particle diffusion. As they act in series, the slower one of the two would be the rate-determining step. The intra-particle diffusion varies with the square root of time [20], as shown below:

$$q_t = k_{\mathrm{id}} t^{0.5}, \tag{10}$$

where q_t is the amount adsorbed (mg g^{-1} m) at time t; t is the time (min); and k_{id} is the intra-particle diffusion coefficient (mg g^{-1} min$^{0.5}$).

The k_{id} values were determined from the slope of the linear plot between q_t vs $t^{0.5}$ and the results for different experiments are shown in table 2. From the R^2 values, it can be concluded that the process is controlled by pore diffusion.

The initial curved portion relates to the film diffusion (D_1), and the later linear portion represents the diffusion (D_2) within the adsorbent. Assuming spherical geometry of the adsorbent particles, the relationship between weight uptake and time using Fick's law can be shown as:

$$q_t/q_{\mathrm{e}} = 6(D_1/\pi a^2)^{1/2} t^{1/2} \tag{11}$$

$$\ln(1 - q_t/q_{\mathrm{e}}) = \ln(6/\pi^2) - (D_2 \pi^2 t/a^2). \tag{12}$$

The values of the D_1 (film diffusion) and D_2 (pore diffusion) coefficients are shown in table 2. The large negative values of the same order of magnitude indicate that both film and pore diffusion control the adsorption mechanism.

Table 2. Physical constants for different adsorption parameters.

	Intra-particle diffusion parameters						Isotherm parameter: Langmuir constant			Isotherm parameter: Freundlich constant		
Parameter	k_{id}	R^2	$D_1 \times 10^{-12}$	R^2	$D_2 \times 10^{-12}$	R^2	Q_0	b	R^2	b_f	K_f	R^2
pH												
4.9	0.34	0.98	1.463	0.94	0.262	0.99	23.98	−0.01	0.86	−0.62	843 917.5	0.92
2.98	0.94	0.98	0.478	0.9	0.218	0.95						
2.44	1.28	0.93	0.356	0.84	0.393	0.94						
1.96	2.68	0.97	0.46	0.88	0.298	0.99						
1.7	2.65	0.93	0.604	0.95	0.276	0.95						
Concentration ($mg\,l^{-1}$)												
400	2.48	0.92	0.184	0.9	0.32	0.97	175.4	0.058	0.99	−1.43	6054	0.98
450	2.13	0.8	0.126	0.98	0.473	0.98						
500	2.69	0.93	0.463	0.91	0.284	0.95						
550	2.8	0.95	0.394	0.97	0.291	0.98						
600	3.1	0.96	0.071	0.94	0.284	0.98						
650	3.04	0.95	0.09	0.95	0.313	1						
700	2.78	0.93	0.196	0.98	0.334	0.99						
Adsorbent dose ($g\,l^{-1}$)												
2.4	2.27	0.9	0.151	0.94	11	0.99	232.6	0.013	0.99	3.7	39.25	0.89
2	2.72	0.94	0.463	0.91	33.69	0.97						
1.6	3.07	0.95	0.168	0.99	12.2	0.97						
1.2	3.34	0.97	0.292	1	21.2	0.98						
0.8	3.43	0.85	0.78	0.85	56.71	0.98						
Temperature (°C)												
30	2.69	0.93	0.463	0.91	0.284	0.95	232.6	0.013	0.99	3.7	39.25	0.98
40	2.88	0.96	0.079	0.94	0.262	0.98						
50	2.79	0.97	0.163	0.98	0.254	0.98						
60	3.64	0.93	0.137	0.96	0.356	1						
Particle size (μm)												
53.5	2.69	0.93	0.463	0.91	0.284	0.95	84.75	−0.01	0.99	−0.699	43.91	.989
97.6	2.46	0.85	0.551	0.93	1.596	0.98						
135	2.32	0.89	0.894	0.87	4.496	0.96						
174	2.3	0.88	1.96	0.93	7.365	0.97						
221	1.41	0.86	6.049	0.97	9.8	0.9						

3.11 *Equilibrium studies*

The adsorption isotherm can be explained by two classical mechanisms such as Freundlich and Langmuir, which are represented by equations (13) and (14), respectively:

$$\ln q_e = \ln K_f + b_f \ln C_e, \tag{13}$$

where K_f is the adsorption capacity ($mg\,g^{-1}$), and b_f is the empirical parameter related to the intensity of adsorption.

$$C_e/q_e = 1/Q^\circ b + C_e/Q^\circ, \tag{14}$$

where Q° ($mg\,g^{-1}$), the Langmuir constant, which represents the monolayer adsorption capacity and relates to the heat of adsorption.

Using equations (13) and (14), the constant values were evaluated for various adsorption parameters along with the coefficient of determinant and are shown in Table 3. From the coefficient of determinant and C_e values, it can be concluded that the adsorption isotherm follows both Freundlich and Langmuir models. The Q° value is the maximum value of q_{eq}, which is important to identify which adsorbent shows the highest uptake capacity and, as such, is useful in scaling up. The values vary between 23 and 232 $mg\,g^{-1}$, which compares

Table 3. Comparison with other adsorbents.

Biosorbent	q_{max} (mg l^{-1})	pH	T (°C)	C_0 (mg l^{-1})	Reference
Aeromonas cavae	124.46	2.5	20	5–350	[21]
Chlorella vulgaris	24	2	25	25–250	[22]
Zooglera ramigera	3	2	25	25–400	[22]
Halimeda opuntia	40	4.1	26	25–400	[22]
Rhizopus arrhizus	62	2	25	25–400	[23]
Rhizopus arrhizus	8.8	2	25		[22]
Rhizopus nigrificans	123.45	2	25	50–500	[24]
Sargassum	40	2			[25]
Spirogyra	14.7	2	18	25–400	[26]
Pinus sylvestris	201.81	1	25	50–300	[27]
Salvinia cucullata	232	1.7	30	500	Current studies

well with other biosorbents, as shown in table 3. Although it is not possible to compare the results with other adsorbents due to varying experimental conditions, it can be concluded that the present adsorbent is efficient in treating Cr(VI)-contaminated water.

4. Conclusions

(1) The rate of adsorption increased with an increase in agitation speed up to 600 rpm. After 600 rpm the increase was marginal.
(2) The rate of adsorption may be due to both surface diffusion and intra-particle diffusion.
(3) The adsorption efficiency increased with decreasing pH, which may be due to protonation of the adsorbent that facilitates the adsorption of anions like Cr(VI).
(4) The higher adsorbent concentration increases the percentage of adsorption, whereas a reverse trend was observed in the case of uptake. The increase in adsobate concentration decreased the percentage of adsorption.
(5) The kinetics of adsorption followed a pseudo-second-order model.
(6) The low activation energy suggested that the adsorption process followed a diffusion-controlled mechanism.
(7) From the maximum uptake values, it can be concluded that the present adsorbent can be used as a potential adsorbent to treat Cr(VI)-contaminated water.
(8) The rate-determining step is observed to be controlled by intraparticle diffusion.

Acknowledgements

The authors thank the Director, RRL, Bhubaneswar for his kind permission to publish this paper. One of the authors, Saroj Sundar Baral, thanks CSIR, New Delhi for providing financial assistance.

References

[1] M. Erdam, H.S. Altundagan, F. Tumen. Removal of hexavalent chromium by using heat activated bauxite. *Min. Eng*., **17**, 1045–1052 (2004).
[2] Y.C. Sarma. Cr(VI) from industrial effluents by adsorption on an indigenous low cost material. *Colloid Surf. A. Phyiochem. Eng. Aspects*., **215**, 155–162 (2003).
[3] A. Lu, S. Zhong, J. Chen, J. Shi, J. Tang, X. Lu. Removal of Cr(VI) and CR(III) from aqueous solutions and industrial wastewaters by natural clino-pyrrhotite. *Environ. Sci. Technol*., **40**, 3064–3069 (2006).
[4] V.K. Garg, R. Gupta, R. Kumar, R.K. Gupta. Adsorption of Cr from aqueous solution on treated sawdust. *Bioresour. Tech*., **92**, 79–81 (2004).

[5] J. Pradhan, S.N. Das, R.S. Thakur. Adsorption of hexavalent chromium from aqueous solution by using activated red mud. *J. Colloid Interf. Sci*., **217**, 137–141 (1999).
[6] D.D. Das, R. Mohapatra, J. Pradhan, S.N. Das, R.S. Thakur. Adsorption of Cr(VI) from aqueous solution using activated cow dung carbon. *J. Colloid Interf. Sci*., **232**, 235–240 (2000).
[7] V. Sarin, K.K. Pant. Removal of chromium from industrial waste by using eucalyptus bark. *Bioresour. Technol*., **97**, 15–20 (2005).
[8] K.K. Singh, R. Rastogi, S.H. Hasan. Removal of Cr(VI) from wastewater using rice bran. *J. Colloid Interf. Sci*., **290**, 61–68 (2005).
[9] M. Kobya, E. Demirbas, E. Senturk, M. Ince. Adsorption of heavy metal ions from aqueous solutions by activated carbon prepared from apricot stone. *Bioresour. Technol*., **96**, 1518–1521 (2005).
[10] J. Bajpai, R. Shrivastava, A.K. Bajpai. Dynamic and equilibrium studies on adsorption of Cr(VI) ions onto binary bio-polymeric beads of cross linked alginate and gelatin. *Colloids Surf. A: Physicochem. Eng. Aspects*, **236**, 81–90 (2004).
[11] M. Dakiky, M. Khamis, A. Manassra, M. Mereb. Selective adsorption of chromium(VI) in industrial wastewater using low-cost abundantly available adsorbents. *Adv. Environ. Res*., **6**, 533–540 (2002).
[12] L. Chun, C. HongZhang, L. ZuoHu. Adsorptive removal of Cr(VI) by Fe-modified steam exploded wheat straw. *Process Biochem*., **39**, 541–545 (2004).
[13] S. Goldberg, G. Sposito. The mechanism of specific phosphate adsorption by hydoxilated mineral surface: A review. *Common Soil Sci. Plant Anal*., **16**, 824–833 (2003).
[14] H.S. Attundogar, S. Attundogar, M. Bildik, F. Tumen. Arsenic adsorption from aqueous solution by activated red mud. *Waste Manage*., **22**, 357–363, 2002).
[15] H.S. Attundogar, F. Tumen. Removal of phosphate from aqueous solution by using Bauxite: The activated sludge. *J. Chem. Technol. Biotech*., **78**, 824–833 (2003).
[16] L.D. Benefield, J.P. Judkins, B.L. Wend. *Process Chemistry for Water and Waste Water Treatment*, Prentice-Hall, Englewood Cliffs, NJ (1982).
[17] N.K. Hamidi, X.D. Chen, M.M. Farid, M.G.Q. Lu. Adsorption kinetics for the removal of Cr(VI) from aqueous solution by adsorbent derived from used tyre and sawdust. *Chem. Eng. J*., **84**, 95–1005 (2001).
[18] N. Tewari, P. Vasudevan, B.K. Gupta. Study on biosorption of Cr(VI) by *M. hiemalis. Biochem. Eng. J*., **23**, 185–192 (2005).
[19] B.S. Inbaraj, N. Sulochana. Basic dye adsorption on a low cost carbonaceous sorbent – kinetic and equilibrium studies. *Ind. J. Chem. Tech*., **9**, 201–208 (2002).
[20] T. Karthikeyan, S. Rajgopal, L.R. Miranda. Cr(VI) adsorption from aqueous solution by *Hevea brasilinesis* sawdust activated carbon. *J. Hazard. Mater*., **124**, 192–199 (2005).
[21] M.X. Loukidou, A.I. Zouboulis, T.D. Karapantsios, K.A. Matis. Equilibrium and kinetic modeling of Cr(VI) biosorption by *Aeromonas caviae. Colloids Surf. A: Physicochem. Eng. Aspects*, **242**, 93–104 (2004).
[22] F. Veglio, F. Beolcini. Removal of metals by biosorption: A review. *Hydrometallurgy*, **44**, 301 (1997).
[23] S. Prakasan, J.S. Merre, R. Sheela, N. Saswati, S. Ramakrisna. Biosorption of chromium VI by free and immobilized *Rhizopus arrhizus. Environ. Pollut*., **104**, 421 (1999).
[24] T.E. Abraham. Studies on enhancement of Cr(VI) biosorption by chemically modified biomass of *Rhizopus nigricans. Wat. Res*., **36**, 1224 (2002).
[25] D. Kratochvil, P. Pimentel, B. Volesky. Removal of trivalent and hexavalent chromium by seaweed biosorbent. *Environ. Sci. Technol*., **32**, 2693 (1998).
[26] D. Kratochvil, P. Pimentel. Advances in the biosorption of heavy metals. *Trends Biotechnol*., **16**, 291 (1998).
[27] H. Ucun, Y.K. Bayhan, Y. Kaya, A. Chikici, O.F. Algur. Biosorption of chromium(VI) from aqueous solution by cone biomass of *Pinus sylvestris. Bioresour. Technol*., **85**, 155 (2002).